Liquid Crystals
Publication details, including instructions for authors and subscription information:
http://www.informaworld.com/smpp/title~content=t713926090

Critical heat capacity variation at the smectic A_1-smectic A_2 transition

C. W. Garland[a]; C. Chiang[a]; F. Hardouin[b]
[a] Department of Chemistry and Center for Materials Science and Engineering, Massachusetts Institute of Technology, Cambridge, Massachusetts, U.S.A. [b] Centre de Recherche Paul Pascal, Université de Bordeaux I, Domaine Universitaire, Talence Cedex, France

To cite this Article Garland, C. W. , Chiang, C. and Hardouin, F.(1986) 'Critical heat capacity variation at the smectic A_1-smectic A_2 transition', Liquid Crystals, 1: 1, 81 — 86
To link to this Article: DOI: 10.1080/02678298608086492
URL: http://dx.doi.org/10.1080/02678298608086492

LIQUID CRYSTALS, 1986, VOL. 1, NO. 1, 81–86

Critical heat capacity variation at the smectic A_1–smectic A_2 transition

by C. W. GARLAND and C. CHIANG
Department of Chemistry and Center for Materials Science and Engineering, Massachusetts Institute of Technology, Cambridge, Massachusetts 02139, U.S.A.
and F. HARDOUIN
Centre de Recherche Paul Pascal, Université de Bordeaux I, Domaine Universitaire, 33405 Talence Cedex, France

(*Received 29 October 1985; accepted 27 November 1985*)

A high resolution a.c. calorimetric study has been carried out on a mixture of 4-n-hexylphenyl-4′-(4″-cyanobenzoyloxy)benzoate (DB_6) and terephthalylidene-bis-(4-n-butylaniline) (TBBA). The heat capacity at the smectic A_1–smectic A_2 (S_{A_1}–S_{A_2}) transition in a DB_6 + 15 per cent TBBA mixture exhibits a distinct cusp with a critical exponent $\alpha \simeq -0{\cdot}15$. This value for α is consistent with the critical correlation exponent ν obtained from X-ray scattering, but it does not conform with current theoretical predictions that the S_{A_1}–S_{A_2} transition should belong to the Ising universality class.

Recent studies carried out at Bordeaux and Orsay have led to the discovery and structural characterization of several new smectic A phases [1]. These new liquid crystal structures occur in polar molecules with long aromatic cores containing three phenyl rings. Mixtures of 4-n-hexylphenyl-4′-(4″-cyanobenzoyloxy)benzoate (DB_6) and terephthalylidene-bis-(4-n-butylaniline) (TBBA) are of particular interest since they exhibit both smectic A_1(S_{A_1}) and smectic A_2(S_{A_2}) phases [2]. For mixtures with a TBBA mole fraction in the range $\sim 0{\cdot}12$ to $\sim 0{\cdot}24$, the sequence nematic(N)–S_{A_1}–S_{A_2} is observed on cooling. According to X-ray studies [3, 4], all three phases exhibit scattering associated with *two* commensurate wavevectors $q_z : q_1 = 2\pi/2L$ and $q_2 = 2\pi/L = 2q_1$. Figure 1 shows a schematic representation of the S_{A_1} and S_{A_2} phases that can be formed by polar molecules of length L. Note that TBBA is non-polar but has a molecular length almost equal to that of DB_6. The S_{A_1} phase is a single-layer smectic with layer thickness L (leading to a quasi-Bragg peak at q_2) and fluctuation scattering at q_1 associated with cybotactic bilayer groups. The S_{A_2} phase involves a commensurate condensation of quasi-Bragg peaks at both q_1 and q_2. The nematic phase exhibits diffuse scattering at q_1 and q_2 due to fluctuations.

The S_{A_1}–S_{A_2} transition is of interest since current theoretical models predict that this transition should be in the Ising universality class [5, 6]. The heat capacity results reported here yield a critical exponent, $\alpha \simeq -0{\cdot}15$. This does not conform to the expected Ising behaviour but is consistent with the correlation exponent obtained from recent high resolution X-ray studies [4].

The a.c. calorimeter used in this investigation has been described previously [7]. The measured heat capacity, C_p(obs), corresponds to the total heat capacity of a sealed cell weighing $\sim 0{\cdot}6$ g, of which 52·7 mg is due to the liquid crystal sample. The measured heat capacity of the empty cell, C_p(empty), varied linearly from 0·191 J/K

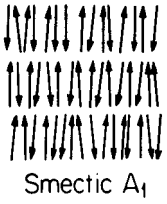

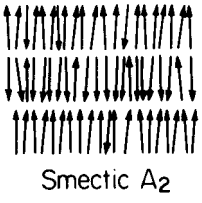

Figure 1. Schematic representation of the S_{A_1} and S_{A_2} phases in polar liquid crystals.

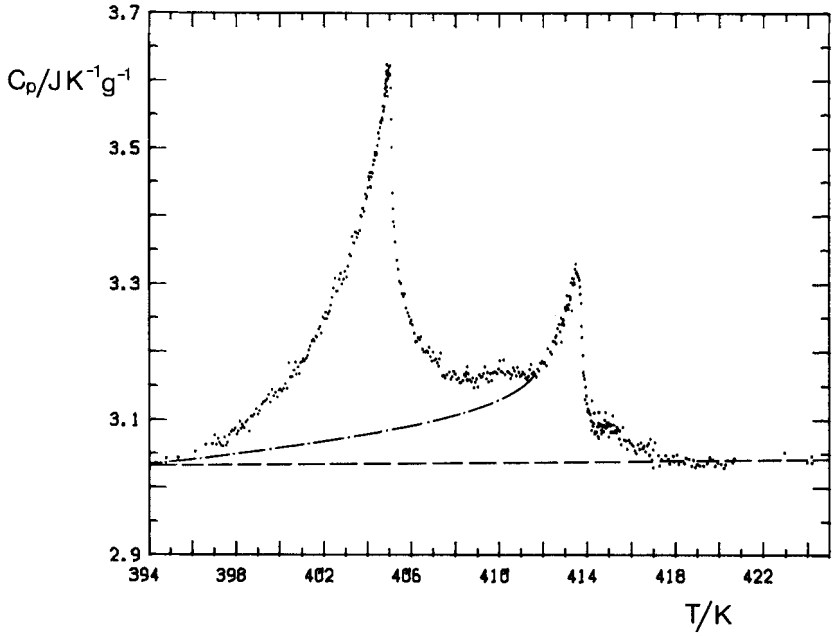

Figure 2. Specific heat of DB_6 + 15 per cent TBBA. The dashed line shows the linear C_p(background) variation, which has a slope of 0·00034/J K^{-2} g^{-1}. The dot–dash curve indicates the estimated C_p(baseline) formed by the tail of the N-S_{A_1} peak; this curve has a slope of 0·005/J K^{-2} g^{-1} at T_c.

at 395 K to 0·196 J/K at 420 K; thus C_p(empty) is roughly one-half of C_p(obs), which varied from 0·350 to 0·385 J/K. The reported results are specific heats determined from

$$C_p = [C_p(\text{obs}) - C_p(\text{empty})]/W, \quad (1)$$

where W is the weight of the liquid crystal sample. The sample studied was a

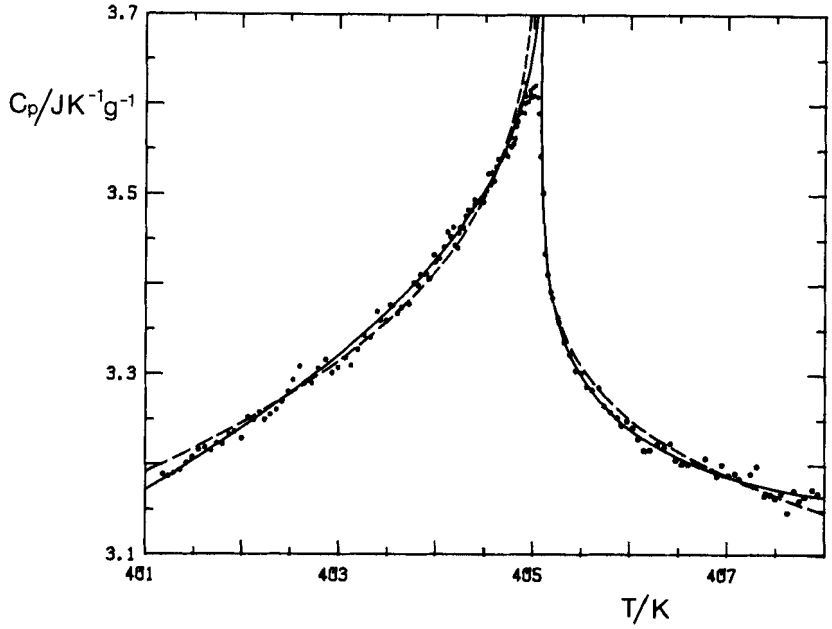

Figure 3. Specific heat near the S_{A_1}–S_{A_2} transition. The temperature range shown here is range 1 used in the analysis. The smooth curves correspond to fits of the data with equation (2). The dashed line represents fit 3 (the Ising exponent $\alpha = 0{\cdot}11$), and the solid line represents fit 4 ($\alpha = -0{\cdot}15$).

DB_6 + TBBA mixture with a TBBA mole fraction of $\sim 0{\cdot}15$. This sample was prepared at Domaine University, and the measurements were carried out at MIT.

The variation of the heat capacity over a wide temperature range is given in figure 2. These data allow us to estimate the linear C_p(background) which dominates the behaviour away from the phase transitions. We have also estimated the baseline under the S_{A_1}–S_{A_2} peak caused by the low temperature tail of the N-S_{A_1} peak. This excess heat capacity associated with the N-S_{A_1} transition has been discussed elsewhere together with the recent N-S_{A_1} results on alkoxybenzoyloxy cyanostilbenes [8]. The detailed critical variation in C_p near the S_{A_1}–S_{A_2} transition is shown in figure 3. Several runs carried out over a long period of time (~ 80 hours) indicate that the critical temperature T_c for this transition undergoes a slow linear drift of $-16{\cdot}5$ mK/h. A correction has been made for this T_c drift, but it should be noted that such a drift does not affect the value of the critical exponent α.

The data analysis was carried out using the expression

$$C_p^{\pm} = A^{\pm}|t|^{-\alpha}(1 + D^{\pm}|t|^{0{\cdot}5}) + B + E(T - T_c), \qquad (2)$$

where $t \equiv (T - T_c)/T_c$ is the reduced temperature and the superscripts $+$, $-$ denote $T > T_c$ or $T < T_c$. The values of the parameters were obtained by simultaneously fitting data above and below T_c with the scaling constraints $\alpha^+ = \alpha^- = \alpha$ and $B^+ = B^- = B$. The non-critical slope E can be taken as a free parameter, but we have usually preferred to fix E at two physically reasonable values: $E = 0{\cdot}005\,\mathrm{J\,K^{-2}g^{-1}}$ (corresponding to the slope at T_c of the dot–dash curve in figure 2) and $E = 0{\cdot}00034\,\mathrm{J\,K^{-2}g^{-1}}$ (corresponding to the slope of the dashed line in figure 2). There is no significant difference in the quality or character of these fits, and

Critical parameters for the S_{A_1}–S_{A_2} transition obtained from fits with equation (2) to data over two reduced temperature ranges (see text). Parentheses indicate that the parameter was held fixed at the given value. The values of χv^2 are based on the choice of a constant standard deviation $\sigma_i = 0{\cdot}007$ for all the data points.

Fit	Range	T_c/K	α	A^+/J K^{-1} g^{-1}	A^-/J K^{-1} g^{-1}	B/J K^{-1} g^{-1}	D^+	D^-	$10^3 E$/J K^{-2} g^{-1}	χv^2
1*A*	1	405·062	−0·126	−1·750	−0·9856	4·014	−0·92	4·87	(5)	1·38
1*B*	1	405·062	−0·137	−1·801	−0·9578	3·975	−1·32	5·68	(0·34)	1·38
2*A*	2	405·062	−0·155	−1·849	−0·9001	3·910	−1·37	6·33	(5)	1·23
2*B*	2	405·063	−0·160	−1·892	−0·8883	3·896	−1·73	7·13	−1·05	1·25
3	1	405·060	(0·11)	0·1367	0·2576	3·125	−11·35	−7·90	(5)	3·50
4	1	405·060	(−0·15)	−1·899	−0·9922	3·947	−1·41	5·16	(5)	1·39
5	1	405·013	(−0·35)	−5·483	−2·2211	3·739	−4·81	2·43	(5)	2·38
6	2	405·064	(0·11)	0·1448	0·2426	3·112	−11·78	−5·83	(5)	1·55
7	2	405·062	(−0·15)	−1·826	−0·9134	3·924	−1·28	5·99	(5)	1·21
8	2	405·060	(−0·35)	−5·287	−0·8406	3·679	−6·11	26·71	(5)	1·62

most of the fits reported here are those obtained with $E = 0{\cdot}005\,\mathrm{J\,K^{-2}\,g^{-1}}$. Fits were carried out over two temperature ranges. The data set for range 1 contained 141 points between 401·17 K and 407·93 K ($-9{\cdot}6 \times 10^{-3} < t < 7 \times 10^{-3}$) and that for range 2 contained 70 points between 403·83 K and 406·34 K ($-3{\cdot}0 \times 10^{-3} < t < 3{\cdot}2 \times 10^{-3}$). In both cases, data points between 404·887 K and 405·077 K were omitted because of a pronounced rounding of the heat capacity peak very close to T_c.

A variety of least-squares fits with equation (2) are shown in the table. Four of these fits (1*A*, 1*B*, 2*A*, 2*B*) were carried out with the critical exponent α taken as a freely adjustable parameter. The resulting α values are all negative and lie between $-0{\cdot}126$ and $-0{\cdot}160$. Fits 1*B* and 2*B* illustrate the fact that changing the value of the slope E has very little effect on the other parameters. Fits 3–5 allow a comparison of the quality of fits over range 1 with α fixed at 0·11 (the Ising value), $-0{\cdot}15$ (an effective best value), and $-0{\cdot}35$ (a stronger cusp). These can also be compared with fits 6–8, where the same fixed α values are used in fitting the data in range 2. The use of fixed α values allows us to test the effect of range shrinking on the values of T_c, $A^{\pm}$, B, and $D^{\pm}$. The parameters for fits with α set equal to 0·11 and $-0{\cdot}15$ were quite stable on range shrinking, whereas A^- and D^- changed dramatically for the two fits with α set at $-0{\cdot}35$.

On the basis of the reduced chi-squared values given in the table, we conclude that a negative α value of $-0{\cdot}15$ provides a significantly better fit to these data than does the theoretically expected Ising value of $+0{\cdot}11$. This conclusion, which is based on the F test, can be supported with better than 99 per cent confidence limits for range 1 [$\nu = 135$, $F_{0{\cdot}01}(135, 135) = 1{\cdot}50$ compared to $\chi\nu^2(\text{fit } 3)/\chi\nu^2(\text{fit } 4) = 2{\cdot}52$] and with 80 per cent confidence limits for range 2 [$\nu = 64$, $F_{0{\cdot}2}(64, 64) = 1{\cdot}23$ compared to $\chi\nu^2(\text{fit } 6)/\chi\nu^2(\text{fit } 7) = 1{\cdot}28$]. Furthermore, it should be noted that figure 3 shows a clear systematic pattern for the deviations from the Ising fit whereas the deviations from the $\alpha = -0{\cdot}15$ fit are both smaller and random. It is difficult to assess the error-bound on the best α value, but we estimate that $\alpha = -0{\cdot}15 \pm 0{\cdot}10$ represents 90 per cent confidence limits.

Such a negative heat-capacity exponent (corresponding to a finite cusp in C_p) should be considered in the context of the critical exponents obtained in a recent X-ray investigation of the DB_6 + TBBA system. Chan *et al.* [4] report $\gamma = 1{\cdot}46 \pm 0{\cdot}05$ for the susceptibility exponent and $\nu_{\parallel} = \nu_{\perp} = 0{\cdot}74 \pm 0{\cdot}03$ for the correlation length exponents parallel and perpendicular to the director. Thus, two independent experiments reveal a S_{A_1}–S_{A_2} critical behaviour that disagrees with the predicted Ising behaviour ($\alpha_I = 0{\cdot}11$, $\nu_I = 0{\cdot}63$, $\gamma_I = 1{\cdot}24$) [9]. The two experiments are consistent with each other in the sense that the hyperscaling relation $\alpha + 3\nu = 2$ is obeyed within the estimated error limits ($\alpha + 3\nu = 2{\cdot}07 \pm 0{\cdot}19$).

It might be noted that the observed critical exponents are in fairly reasonable empirical agreement with so-called Fisher renormalized Ising behaviour: $\alpha_R = -\alpha_I/(1 - \alpha_I) = -0{\cdot}124$, $\nu_R = \nu_I/(1 - \alpha_I) = 0{\cdot}71$, $\gamma_R = \gamma_I/(1 - \alpha_I) = 1{\cdot}39$ [10]. However, it is unclear whether any hidden variable subject to a constraint (such as an impurity in a fluid near its liquid–vapour critical point) exists in the DB_6 + TBBA system. Further experimental work on DB_6 + TBBA mixtures with other compositions is in progress, and it is hoped to confirm and refine the characterization of the thermal fluctuation behaviour near the S_{A_1}–S_{A_2} transition.

This work was supported in part by the National Science Foundation under contract DMR 83–15637.

References

[1] HARDOUIN, F., LEVELUT, A. M., ACHARD, M. F., and SIGAUD, G., 1983, *J. Chim. phys.*, **80**, 53, and references cited therein.

[2] SIGAUD, G., HARDOUIN, F., ACHARD, M. F., and GASPAROUX, H., 1979, *J. Phys., Paris*, **40**, C3-356.

[3] HARDOUIN, F., LEVELUT, A. M., BENATTAR, J. J., and SIGAUD, G., 1980, *Solid-st. Commun.*, **33**, 337. HARDOUIN, F., LEVELUT, A. M., and SIGAUD, G., 1981, *J. Phys., Paris*, **42**, 107. LEVELUT, A. M. (private communication).

[4] CHAN, K. K., 1984, Ph.D. thesis, Harvard University. CHAN, K. K., PERSHAN, P. S., SORENSEN, L. B., and HARDOUIN, F., 1985, *Phys. Rev. Lett.*, **54**, 1694.

[5] PROST, J., 1979, *J. Phys., Paris*, **40**, 581. PROST, J., 1980, *Liquid Crystals of One- and Two-Dimensional Order* (Springer Series in Chemical Physics, Vol. 11) (Springer-Verlag), p. 125.

[6] WANG, J., and LUBENSKY, T. C., 1984, *Phys. Rev.* A, **29**, 2210.

[7] MEICHLE, M., and GARLAND, C. W., 1983, *Phys. Rev.* A, **27**, 2624. SANCHEZ, G., MEICHLE, M., and GARLAND, C. W., 1983, *Phys. Rev.* A, **28**, 1647.

[8] CHIANG, C., and GARLAND, C. W., 1985, *Molec. Crystals liq. Crystals*, **122**, 25.

[9] LEGUILLON, J. C., and ZINN-JUSTIN, J., 1977, *Phys. Rev. Lett.*, **39**, 95; 1980, *Phys. Rev.* B, **21**, 3976.

[10] FISHER, M. E., 1968, *Phys. Rev.*, **176**, 257. FISHER, M. E., and SCESNEY, P. E., 1970, *Phys. Rev.* A, **2**, 825.